Optical beam instabilities in nonlinear nanosuspensions

R. El-Ganainy,[1] D. N. Christodoulides,[1] Ziad H. Musslimani,[2] C. Rotschild,[3] and M. Segev[3]

[1]College of Optics & Photonics–CREOL, University of Central Florida, Orlando, Florida 32816, USA
[2]Department of Mathematics, Florida State University, Tallahassee, Florida 32306-4510, USA
[3]Physics Department, Technion–Israel Institute of Technology, Haifa 32000, Israel

Received July 30, 2007; revised September 27, 2007; accepted September 28, 2007;
posted October 1, 2007 (Doc. ID 85904); published October 26, 2007

We investigate the modulation instability of plane waves and the transverse instabilities of soliton stripe beams propagating in nonlinear nanosuspensions. We show that in these systems the process of modulational instability depends on the input beam conditions. On the other hand, the transverse instability of soliton stripes can exhibit new features as a result of 1D collapse caused by the exponential nonlinearity.

OCIS codes: 190.4420, 190.3970.

Over the last two decades the mechanical interaction between light and dielectric nanoparticles has received considerable attention and has led to the emergence of new tools in optics such as optical tweezers and traps [1–5]. The nonlinear Kerr-like character of this process was recognized in a series of publications starting with the pioneering work of Ashkin *et al.* [6–11]. Lately, two independent theoretical studies have shown that the interplay between the optical and thermodynamic forces in nanosuspensions leads to exponential nonlinearities [12–14]. As noted in Refs. [12,13], even though these exponential nonlinearities are always of the self-focusing type, two different regimes can be distinguished based on the refractive index contrast between the nanoparticles and the host medium. Both beam self-trapping (solitons) as well as self-induced transparency effects were predicted in such configurations [13].

In this Letter we consider optical beam instabilities in nanocolloidal systems. Depending on the regime, the modulational instability (MI) behavior can display either Kerr or non-Kerr characteristics. Transverse MI of soliton stripe beams is also investigated, and a new instability is identified as a result of the 1D collapse caused by the exponential nonlinearity.

We start our analysis by writing the evolution equation for an optical beam propagating in a nanoparticle colloidal system [13]:

$$i\frac{\partial\varphi}{\partial z}+\frac{1}{2k_0n_b}\nabla_\perp^2\varphi+k_0(n_p-n_b)V_p\rho_0\times\exp\left(\frac{\alpha}{4k_BT}(|\varphi|^2-|\varphi_0|^2)\right)\varphi+\frac{i}{2}\sigma\rho_0\exp\left(\frac{\alpha}{4k_BT}|\varphi|^2\right)\varphi=0. \quad (1)$$

Here φ is the electric field envelope, k_BT is the thermal energy, α is the particle polarizability [13], n_p and n_b are the particle and the background (host medium) refractive indices, respectively, and V_p is the particle volume. In addition, k_0 is the free space wavenumber and ρ_0 is the unperturbed particle concentration (in the absence of any illumination). In this equation φ_0 represents a possible infinite light background or a plane-wave component (if it exists) upon which the beam rests. This term arises from the integration of the Nernst–Planck equation $(\alpha/4k_BT)\rho\nabla|\varphi|^2-\nabla\rho=0$ [13], which leads to $(\alpha/4k_BT)\times(|\varphi|^2-|\varphi_0|^2)=\ln(\rho/\rho_0)$. By rearranging, one obtains the nonlinear term appearing in Eq. (1). It is worth noting that this model describes only diluted suspensions (with typical filling factors below ~0.3%) and hence particle–particle interactions can be ignored. Note that for very dense colloidal systems the nonlinear Rayleigh losses described by the last term in Eq. (1) [13] (with σ being the scattering cross-section) dominate the dynamics and greatly suppress nonlinear effects. In normalized units, Eq. (1) takes the form [13]

$$i\frac{\partial u}{\partial\xi}+u_{XX}+u_{YY}+a\exp[a(|u|^2-b|u_o|^2)]u+i\delta\exp(a|u|^2)u=0, \quad (2)$$

where $\varphi=(4k_BT/|\alpha|)^{1/2}u$, $\xi=z/(2k_0n_bw^2)$, $X=x/w$, $Y=y/w$, and the spatial scale w is given by $w^{-2}=2k_0^2n_b|n_p-n_b|V_p\rho_0$. In Eq. (2), δ is a normalized loss coefficient. Note that Eq. (2) was written in a general form to account for different scenarios. The case $a=+1$ corresponds to a system with an index contrast m greater than unity $(m=n_p/n_b>1)$, while $a=-1$ is used for $m<1$. The constant b is either 1 or 0 depending on whether the input is a plane wave (or rests on a plane wave) that covers the entire cell or a quasi-plane-wave broad beam that covers only a small portion of the cell, respectively.

We first consider the process of MI in the absence of scattering losses. To do so we write the plane-wave solution of Eq. (2) as $u=u_o\exp(i\mu\xi)$, where $\mu=a\exp(a(1-b)u_o^2)$. By introducing a small perturbation $\varepsilon(X,\xi)$ in this solution $u=(u_o+\varepsilon(X,\xi))\exp(i\mu\xi)$ and by substituting this latter form back into Eq. (2), then to first order in ε we get

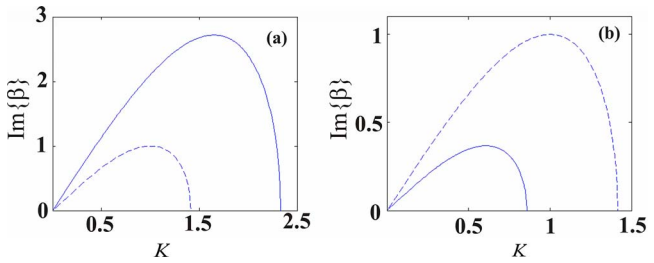

Fig. 1. (Color online) MI gain versus perturbation wavenumber for (a) an exponentially nonlinear ($n_p/n_b>1$) and (b) an exponentially saturable nonlinear nanosuspension system ($n_p/n_b<1$) for the parameters given in the text. The solid/dotted curves depict the MI gain when $b=0/b=1$ for $u_o=1$.

$$i\varepsilon_\xi + \varepsilon_{XX} + u_o^2(\varepsilon+\varepsilon^*)\exp(a(1-b)u_o^2) = 0. \tag{3}$$

Assuming a solution of the form $\varepsilon = A\cos(\beta\xi - KX) + iB\sin(\beta\xi - KX)$, and by eliminating the arbitrary constants A, B, we obtain

$$\beta^2 = K^2[K^2 - 2u_o^2\exp(a(1-b)u_o^2)]. \tag{4}$$

From Eq. (4) we see that under plane-wave excitation conditions ($b=1$) the MI of this system exhibits a Kerr response [15,16] regardless of the refractive index contrast. On the other hand, for the more realistic case of a quasi-plane-wave input, when the beam is wide enough to avoid appreciable diffraction but does not cover the entire cell ($b=0$), the situation is different. In this latter case, when the particle polarizability is positive ($m>1$), Eq. (4) becomes $\beta^2 = K^2(K^2 - 2u_o^2 e^{u_o^2})$. Here, as in the case of Kerr nonlinearities, the maximum gain happens to be at the peak intensity of the beam ($u_{o\,\max}$) and the spatial frequency at which this maximum gain is attained occurs at $K^2 = u_o^2\exp(u_o^2)$. Figure 1(a) shows the gain curve for a system of polystyrene nanoparticles ($n_p = 1.56$) of radius ($r=50$ nm) suspended in water when the particle concentration $7\times10^{17}\,\mathrm{m}^{-3}$. For this set of parameters, the power density of the incident plane wave is $1\,\mathrm{MW/cm}^2$. Conversely, when the particle polarizability is negative ($m<1$), the MI exhibits entirely different characteristics as the dispersion relation takes the form $\beta^2 = K^2(K^2 - 2u_o^2 e^{-u_o^2})$. In this case, in contrast to the previous one, the maximum gain does not monotonically increase with the peak intensity u_o. In fact the maximum intensity occurs when $u_o=1$ at a spatial frequency $K=1/e$. The gain curve in Fig. 1(b) was obtained for "nanobubbles" (with $n_p \approx 1$) of 50 nm radius suspended in water at a concentration of $2\times10^{18}\,\mathrm{m}^{-3}$ (the power density is $0.7\,\mathrm{MW/cm}^2$). In all the examples considered in this paper the wavelength is taken to be $\lambda_0 = 0.532\,\mu$m.

Next we consider the transverse MI of soliton stripes (along y) [17] in the absence of Rayleigh losses. In this case we assume a solution of the form $u = (u_s(X) + \varepsilon(X,Y,\xi))\exp(i\kappa\xi)$, where $u_s(X)$ is a 1D soliton solution of Eq. (2), $\varepsilon(X,Y,\xi)$ is a small perturbation and κ is the soliton eigenvalue. In this case $u_s(\infty)=0$, and hence $\varphi_0=0$. Substituting this latter form in Eq. (2) and by retaining only first-order terms in ε we get

$$i\varepsilon_\xi - \kappa\varepsilon + \varepsilon_{XX} + \varepsilon_{YY} + a\exp(au_s^2)\varepsilon + u_s^2\exp(au_s^2)(\varepsilon+\varepsilon^*) = 0. \tag{5}$$

If in turn we assume

$$\varepsilon(X,Y,\xi) = (V(X)+W(X))\exp[i(\beta\xi + qY)] + (V^*(X) - W^*(X))\exp[-i(\beta^*\xi + qY)], \tag{6}$$

then from Eq. (5) we obtain the following linear coupled eigenvalue equations:

$$V_{XX} + [a\exp(au_s^2) + 2u_s^2\exp(au_s^2) - \kappa - q^2]V = \beta W, \tag{7a}$$

$$W_{XX} + [a\exp(au_s^2) - \kappa - q^2]W = \beta V. \tag{7b}$$

For any specific power level (corresponding to a certain soliton solution u_s), the above generalized eigenvalue problem can be solved for each transverse spatial frequency q. The solution $u_s(X)$ is stable against transverse modulation perturbations when β is real, and it becomes unstable in the complex β domain.

We first consider the case when the particle's refractive index is higher than that of the background, i.e., when $a=1$. In this case, as demonstrated in Ref. [13], the soliton solution has two regimes of stability with respect to longitudinal perturbations (along x) of the form $\varepsilon(X,\xi)$ (Vakhitov–Kolokolov criterion). The transverse instability $\beta-q$ gain curve corresponding to a 1D soliton that belongs to the stable region [13] ($\kappa<2.49$) is shown in Fig. 2(a), where we have used the same parameters as in Fig. 1(a). This gain curve was obtained for a soliton solution of Eq. (2) at a linear power density of 1.3 kW/cm and at $\kappa=1.7$. From Fig. 2(a) one can see that the solution is marginally stable at $q=0$, unstable for long wavelength perturbations, and becomes stable for $q>1.9$. This behavior qualitatively resembles that encountered in nonlinear Kerr systems [17]. Contrary to this latter case, in the longitudinally unstable region ($\kappa>2.49$), the transverse instability displays new features due to the competition between longitudinal and transverse instabilities. Figure 2(b) shows the gain curve for a

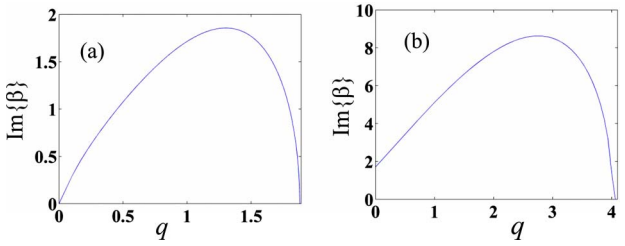

Fig. 2. (Color online) Transverse MI gain of a stripe soliton versus perturbation wavenumber q for an exponentially nonlinear colloidal system when the 1D soliton solution belongs to (a) the stable ($\kappa=1.7$) and (b) the unstable ($\kappa=3$) branch.

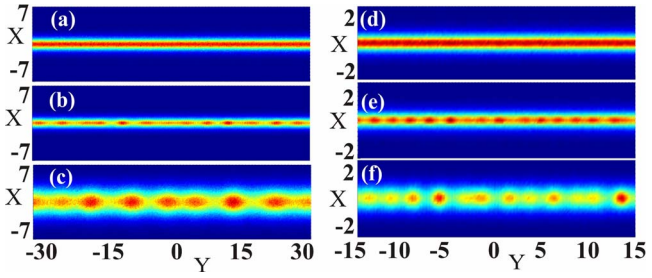

Fig. 3. (Color online) (a)–(c) and (d)–(f): Propagation dynamics of the stripe soliton beams associated with Figs. 2(a) and 2(b), respectively. (a), (d) input profiles. Output intensity in (b) a lossless system at $z=1.9$ mm, (c) in a lossy system (45% of losses at the output) at 6 mm. (e) Output beam in the absence of losses (after 3 mm), and (d) effect of losses (16% after 0.8 mm of propagation).

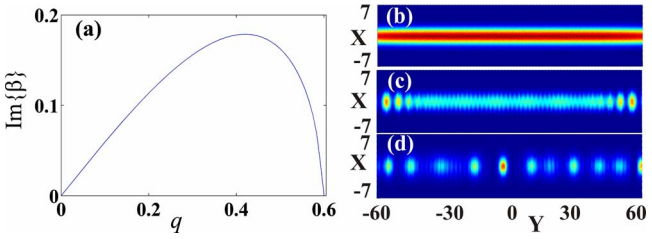

Fig. 4. (Color online) (a) Transverse MI gain of a stripe soliton versus perturbation wavenumber for a saturable exponentially nonlinear colloidal dispersion when $\kappa=0.75$. Corresponding propagation dynamics in this same system after $z=7$ mm for (b) an input soliton stripe beam, when (c) losses are neglected and (d) nonlinear Rayleigh losses are included.

soliton stripe at power density of 1.33 kW/cm and for $\kappa=3$, i.e., when it belongs to the unstable branch of the power-eigenvalue diagram discussed before in Ref. [13]. Note that in this case the soliton stripe beam is unstable even at $q=0$, which might be explained as follows. When $q=0$, the transverse perturbation $\varepsilon(X,Y,\xi)$ described in Eq. (6) effectively reduces to the longitudinal perturbation $\varepsilon(X,\xi)$, which in this specific case is known to be unstable, thus giving rise to a complex eigenvalue solution to the generalized eigenvalue problem of Eq. (7). Figures 3(a)–3(c) depict the propagation dynamics of the stripe soliton corresponding to Fig. 2(a). As clearly seen in Figs. 3(b) and 3(c), transverse instability and filamentation persist even when the Rayleigh losses are included in the simulations. Figures 3(d)–3(f) show what will happen to the stripe beam corresponding to Fig. 2(b) (unstable 1D soliton). In this case, in spite of the scattering losses, the beam quickly disintegrates into collapsing filaments as a result of the synergy of the longitudinal and transverse instabilities. Nonetheless, when the nanoparticles have a negative polarizability (nanoparticles suspended in a higher refractive index host medium), the 1D soliton solution is always stable, and one would expect soliton stripes to be marginally stable at $q=0$, in a way similar to that shown in Fig. 2(a). In fact this prediction is in perfect agreement with linear stability analysis as depicted in Fig. 4(a), where the normalized gain curve corresponds to the nanobubble suspensions considered in Fig. 1(b). The $\beta-q$ diagram in Fig. 4(a) was obtained at a power density of 2.8 kW/cm when $\kappa=0.75$. Figures 4(b)–4(d) show propagation dynamics of a stripe soliton beam [that corresponds to Fig. 4(a)]. In the absence of losses this beam becomes transversely unstable [Fig. 4(c)] starting from the $u=1$ regions where the MI gain is maximum. In Figs. 4(b) and 4(c) these regions are located at the two edges of the finite stripe. Figure 4(d) shows the output beam when the nonlinear Rayleigh losses are included. In this case the filamentations process affects the entire beam more quickly because of self-induced transparency effects [13]. In all previous simulations, to keep the simulation window finite, we use very wide super-Gaussian soliton beams in the y direction as opposed to ideal soliton stripes. This explains the high-frequency dispersive waves that appear in Fig. 4(d) that eventually decay with propagation.

In conclusion we investigated the modulation instability of plane waves and the transverse instabilities of soliton stripe beams propagating in nonlinear nanosuspension systems.

References

1. A. Ashkin, IEEE J. Sel. Top. Quantum Electron. **6**, 841 (2000).
2. D. V. Grier, Nature **424**, 810 (2003).
3. J. P. Gordon, Phys. Rev. A **8**, 14 (1973).
4. A. Ashkin, J. M. Dziedzic, J. E. Bjorkholm, and S. Chu, Opt. Lett. **11**, 288 (1986).
5. K. Dholakia, Nat. Mater. **4**, 579 (2005).
6. P. W. Smith, A. Ashkin, and W. J. Tomlinson, Opt. Lett. **6**, 284 (1981).
7. A. Ashkin, J. M. Dziedzic, and P. W. Smith, Opt. Lett. **7**, 276 (1982).
8. V. E. Yashin, S. A. Chizhov, R. L. Sabirov, T. V. Starchikova, N. V. Vysotina, N. N. Rozanov, V. E. Semenov, V. A. Smirnov, and S. V. Fedorov, Opt. Spectrosc. **98**, 466 (2005).
9. P. J. Reece, E. M. Wright, and K. Dholakia, Phys. Rev. Lett. **98**, 203902 (2007).
10. C. Conti, G. Ruocco, and S. Trillo, Phys. Rev. Lett. **95**, 183902 (2005).
11. C. Conti, N. Ghofraniha, G. Ruocco, and S. Trillo, Phys. Rev. Lett. **97**, 123903 (2006).
12. R. El-Ganainy, K. G. Makris, D. N. Christodoulides, C. Rothchild, and M. Segev, paper QMB4, presented at the Conference on Lasers and Electro-Optics/Quantum Electronics and Laser Science Conference 2007, CLEO/QELS 2007, Baltimore, Maryland, May 6–11, 2007.
13. R. El-Ganainy, D. N. Christodoulides, C. Rotschild, and M. Segev, Opt. Express **15**, 10207 (2007).
14. R. Gordon, J. T. Blakely, and D. Sinton, Phys. Rev. A **75**, 055801 (2007).
15. K. Tai, H. Hasegawa, and A. Tomita, Phys. Rev. Lett. **65**, 135 (1986).
16. D. Kip, M. Soljacic, M. Segev, E. Eugenieva, and D. N. Christodoulides, Science **290**, 495 (2000).
17. E. A. Kuznetsov, A. M. Rubenchik, and V. E. Zakharov, Phys. Rep. **142**, 103 (1986).